NEOPLASIA
www.neoplasia.com

Volume 11 Number 9 September 2009 pp. 921–933 **921**

Transcriptional Regulation of Vascular Endothelial Growth Factor C by Oxidative and Thermal Stress Is Mediated by Lens Epithelium–Derived Growth Factor/p75[1,2]

Batya Cohen*[,3], Yoseph Addadi*[,3], Stav Sapoznik*, Gila Meir*, Vyacheslav Kalchenko†, Alon Harmelin†, Shifra Ben-Dor‡ and Michal Neeman*

*Department of Biological Regulation, The Weizmann Institute, Rehovot 76100 Israel; †Department of Veterinary Resources, The Weizmann Institute, Rehovot 76100 Israel; ‡Biological Services, The Weizmann Institute, Rehovot 76100 Israel

Abstract

Vascular endothelial growth factor C (VEGF-C) plays a critical role in tumor lymphangiogenesis and lymph node metastasis. We report here that VEGF-C expression is regulated by microenvironmental stress including hyperthermia and oxidative stress. Furthermore, we show that this stress response is mediated by transcriptional activation mediated by lens epithelium–derived growth factor (LEDGF/p75). Ectopic expression of LEDGF/p75 in C6 rat glioma and in H1299 human non–small cell lung carcinoma induced VEGF-C expression *in vitro*, whereas in subcutaneous mouse tumor xenografts, LEDGF/p75 stimulated VEGF-C expression and augmented angiogenesis and lymphangiogenesis. Conversely, overexpression of a LEDGF/p75 native antisense or LEDGF/p75–targeted short interfering RNA downmodulated VEGF-C expression. LEDGF seemed to conferred this activity on binding to a conserved stress response element (STRE) located in the *VEGF-C* gene because mutating the STRE was sufficient for the suppression of basal and stress-induced activations of the VEGF-C promoter. Thus, the study reported here identified a role for LEDGF/p75 in stress-regulated transcriptional control of VEGF-C expression. These results provide a possible link for LEDGF/p75 in tumor lymphangiogenesis and cancer metastasis. Hence, our data suggest the LEDGF–VEGF-C axis as a putative biomarker for the detection of stress-induced lymphangiogenesis and LEDGF as a potential target for antimetastatic therapy.

Neoplasia (2009) 11, 921–933

Introduction

Blood and lymphatic vessels provide complementary functions in the maintenance of tissue homeostasis. Blood circulation is optimally designed for efficient delivery and clearance of low–molecular weight nutrients and waste products, as well as the rapid systemic exposure of all tissues to circulating erythrocytes, immune cells, and hormones. The lymphatic system, however, provides a unidirectional route for the clearance of extravasated interstitial fluid, macromolecules, and immune cells from the tissues to the blood circulation through the draining lymph nodes. Both vascular systems were implicated in providing routes for tumor escape and metastatic dissemination.

Development and maintenance of the blood and lymphatic vascular systems are coupled through multiply shared receptors expressed on both lymphatic and blood endothelial cells. Accordingly, angiogenesis and lymphangiogenesis are tightly coregulated, mainly by vascular endothelial growth factors A and C (VEGF-A and -C), two members of the VEGF family. Both VEGF-A and -C induce endothelial cell survival, proliferation, migration, and induction of permeability. VEGF-A predominantly mediates its activity through activation of VEGF receptors 1 and 2 (VEGFR-1 and -2) but not VEGFR-3. VEGF-C is produced as a precursor and undergoes stepwise proteolytic processing, generating 31/29- and 21-kDa fragments with varying affinities for the various VEGF receptors. The mature form of VEGF-C activates

Abbreviations: DLSI, dynamic light scattering imaging; LEDGF, lens epithelium–derived growth factor; STRE, stress response element; VEGF, vascular endothelial growth factor

Address all correspondence to: Prof. Michal Neeman, Department of Biological Regulation, Weizmann Institute, Rehovot 76100 Israel. E-mail: michal.neeman@weizmann.ac.il

[1]This work was supported by the Israel Science Foundation 93/07 (to M.N. and B.C.) and by National Institutes of Health grant R01 CA75334 and the 7th Framework European Research Council Advanced grant 232640-IMAGO (to M.N.). M.N. is incumbent of the Helen and Morris Mauerberger Chair.

[2]This article refers to supplementary materials, which are designated by Figures W1 to W4 and are available online at www.neoplasia.com.

[3]These authors contributed equally to this work.

Received 15 April 2009; Revised 16 June 2009; Accepted 16 June 2009

 1522-8002/09/$25.00
DOI 10.1593/neo.09636

VEGFR-2 on blood endothelial cells. This induces a response similar to that induced by VEGF-A, including increased vascular permeability, proliferation, and migration of vascular endothelial cells but with less potency than VEGF-A [1,2]. VEGF-C, in addition to its angiogenic properties, is a potent inducer of lymphangiogenesis. Binding of the 31/29-kDa protein to VEGFR-3 on lymphatic endothelial cells induces lymphangiogenesis in development, cancer, and wound healing [3,4].

The role of VEGF-C in peritumor lymphatic remodeling and lymph node metastatic spread was demonstrated in a variety of human cancers, including thyroid, prostate, gastric, colorectal, and lung [5,6]. In addition, ectopic stable expression of VEGF-C in cancer cell lines as well as in various mouse tumor models promoted tumor lymphangiogenesis and resulted in an increased incidence of lymph node metastasis [7–9]. In addition to its role in lymphangiogenesis, VEGF-C is secreted in inflammation by cells belonging to the inflammatory progeny [10]. Mice deficient in VEGF-C lack cell sprouting from the cardinal vein and exhibit impaired formation of lymph sacs and edema [3]. Silencing of VEGF-C expression, either by using short hairpin RNA or by applying soluble VEGFR-3, has been shown to inhibit VEGF-C–induced tumor lymphangiogenesis metastasis and enhance survival [11–13].

Maintenance of tissue homeostasis should include mechanism that would augment the functional and structural capacity of the lymphatic bed in response to short- and long-term increased need for lymphatic clearance. Thus, an immediate rise in tissue interstitial pressure pulls the anchoring filaments on the lymphatic endothelial cells, leading to increased permeability and uptake of fluids [14]. We have recently demonstrated, by magnetic resonance imaging, the induction of interstitial convection and lymphatic drain, in response to overexpression of VEGF-A [15–17]. Moreover, VEGF-C expression was demonstrated to be induced by interstitial convection and edema in a number of experimental models [18–20] and in response to inflammation and proinflammatory factors, including tumor necrosis factor α and interleukin 1β [21–23]. Accordingly, various environmental stress signals have been implicated in the induction of VEGF-C expression [24–26]. Recently, it was demonstrated that heparanase induces VEGF-C expression and facilitates tumor xenograft lymphangiogenesis [27].

The aim of this study was to evaluate the molecular basis for regulation of VEGF-C expression by microenvironmental stress signals. A recent study reported that expression of VEGF-C can be induced by the osmosensitive transcription enhancer TonEBP [28]. In the study reported, we present a novel molecular machinery, controlling lymphangiogenesis through the activation of VEGF-C expression. We show here that oxidative stress and hyperthermia augmented VEGF-C expression in the lung tumor H1299 cells. Activation of VEGF-C transcription is conferred by the stress response element (STRE) located in the promoter of VEGF-C through the activity of the transcription factor lens epithelium–derived growth factor (LEDGF)/p75.

LEDGF (designated also as PSIP1 and DFS70 autoantigen) was identified as a survival factor that enhances growth and resistance to cell death induced by oxidative stress, hyperthermia, and serum deprivation [29,30]. LEDGF/p75 was recently implied as a key player in tumor progression and maintenance both in mouse tumor models and in various human cancers [31]. LEDGF was implicated in multiple pathways affecting cancer progression and thus predicts poor survival [32,33]. In addition, it has emerged as an important cellular cofactor involved in tethering of human immunodeficiency virus 1 integrase to chromatin, protecting it from degradation [34]. Indeed, LEDGF is predominately localized to the nucleoplasm of most cell types and is associated with the chromosomes [29]. LEDGF/p75 was reported to bind two different consensus core sequences, namely, heat shock element (HSE) and STRE [35]. However, other studies reported that LEDGF tethers JPO2, a MYC binding protein, to chromatin, affecting transcription in an STRE-independent manner [36,37].

In the study reported here, we demonstrate the role of LEDGF/P75 in inducing tumor VEGF-C expression in response to hyperthermia and oxidative stress. Moreover, human non–small cell lung carcinoma (H1299) and rat glioma (C6) cells with a low basal expression of LEDGF/p75 and VEGF-C were induced to overexpress LEDGF/p75, resulting in an increased production of biologically active VEGF-C and corresponding induction of subcutaneous angiogenesis and lymphangiogenesis.

Materials and Methods

Cell Cultures and Reagents

Cells were cultured in minimum essential medium (human lung cancer A549 cells [ATCC, Manassas, VA] and C6 rat glioma cells [ATCC]), Dulbecco's modified Eagle medium (transformed African green monkey fibroblast cells COS7 [ATCC]), or RPMI (human non–small cell lung carcinoma, H1299 [ATCC]) medium supplemented with 10% fetal bovine serum, penicillin, and streptomycin. All cells were maintained in 5% CO_2/95% air at 37°C.

Reverse Transcription–Polymerase Chain Reaction

Total RNA was extracted from cells using Tri Reagent (Molecular Research Center, Cincinnati, OH). Two micrograms of total RNA was used for first-strand DNA synthesis using SuperScript II RNase H-reverse (Invitrogen, Carlsbad, CA). Polymerase chain reaction (PCR) was performed with the following forward and reverse primers: human VEGF-C (accession no. NM005429: 5′-CTGCTCGCCGCTGCGCTG and 5′-GTGCTGGTGTTCATGCACTGCAG), human LEDGF/p75 (accession no. AFO63020: 5′-CACACAGAGATGATTACTACACTG and 5′-CCATCTTGAGCATCAGATCCTC), mouse, and the native antisense rat LEDGFas (accession nos. AK042735 and CB576984: 5′-CCTGTTGGTTCCTTCTCTAGC and 5′-GGCGGTTCAAAGTCAGTCAAG), human LEDGFas (accession no. AV716383: 5′-CCTGTTTG TTCCTTCTCTAGC and 5′-GGCGATTCAAAGTTAGTC AGG), and human GAPDH (accession no. BC004109: 5′-CGGAGTCAACGGATTTGGTCGTAT and 5′-AGCCTTCTCCATGGTGGTGAAGAC). All PCR conditions and primers were optimized to produce a single product of the correct base pair size in the linear range of the reaction. The target messenger RNA (mRNA) expression level was calculated as the ratio of the target mRNA to GAPDH mRNA for each sample.

Expression Vectors and Stable Transfections

LEDGF and LEDGF antisense (LEDGFas) sequences were reverse-transcribed from H1299 mRNA and PCR-amplified using Phusion high-fidelity DNA polymerase (Finnzymes, Espoo, Finland) together with the following forward and reverse primers: LEDGF, 5′-ATGACTCGCG ATTTCAAACCTGG and 5′-CTAGTTATCTAGGGTAGACTCCTTCAG; LEDGFas, 5′-CCTGTTTGTTCCTTCTCTAGC and 5′-GGCGATTCAAAGTTAGTCAGG. The fragments were ligated into pCR-BluntII-TOPO (Invitrogen), and their sequence fidelity was confirmed by DNA sequence analysis. Inserts were restricted and ligated into pIRES expression vector containing the human EF-1a promoter [38]. Stable transfections were carried out with Lipofectamine 2000 reagent (Invitrogen), and 48 hours after transfection, puromycin (2.5 mg/ml; Sigma, St. Louis, MO) was added to initiate selection. An

average of 50 puromycin-resistant clones was pooled and analyzed for both luciferase activity and LEDGF expression.

Luciferase Reporter Assays

VEGF-C promoter sequence (GenBank accession no. NM-005429) was amplified from human genomic DNA by PCR, using forward (5′-CCGCCGCAGCGCCCGCG) and reverse (5′-GAGAAGAAGCCCAGCAAGTG) primers containing *Bam*HI and *Xho*I restriction sites, respectively. To construct the pVEGF-Cwt-Luc, the product was digested and ligated into pLuc plasmid, which encodes firefly luciferase. The fidelity of the insert was confirmed by DNA sequence analysis. Two mutated pVEGF-C reporter vectors were generated: mutations were introduced into the STRE sequence located within the *VEGF-C* gene using mutated PCR primers (pVEGF-Cm1-Luc, 5′-CACTTCGGGGAAGAAAAGGGAGGAGGGGG; and pVEGF-Cm2-Luc, 5′-GCCAGAGCCCTCGTTTTTCTCCTTTCTTTTCTTCCCCG AAGTG AGAG). For transfections, cells (10^5 per well) were plated in a 24-well plate and transfected 24 hours later with pSV-Renilla (40 ng), luciferase reporter (300 ng), and 500 ng of pIRES alone, pIRES encoding LEDGF/p75 or pIRES encoding LEDGFas, using Lipofectamine 2000 reagent (Invitrogen). Twenty-four hours after transfection, luciferase assay was performed using the dual-luciferase reporter assay system (Promega, Madison, WI). Firefly luciferase activity was normalized to Renilla luciferase activity for each transfected well. For down-modulation analysis of LEDGF/p75 activity, H1299 cells stably expressing pVEGF-Cwt-Luc construct were transfected either with a specific synthetic short interfering RNA (siRNA) targeting nucleotide 1342 to 1361 (5′-AGA CAG CAU GAG GAA GCG dTdT; Dharmacon, Lafayette, CO) [39] or with a nontarget control siRNA (Dharmacon). Forty-eight hours later, cells were stimulated as indicated.

Chromatin Immunoprecipitation Assays

H1299 control cells, or stimulated as indicated, were fixed in 1% formaldehyde for 10 minutes and subjected to chromatin immunoprecipitation (ChIP) assay using the EZ ChIP Chromatin Immunoprecipitation Kit (Upstate Biotechnology, Lake Placid, FL) with anti-LEDGF antibodies (C16; Santa Cruz, Santa Cruz, CA). PCR was performed using primers to amplify the *VEGF-C* promoter (for details, see Luciferase Reporter Assays section). Total genomic DNA amounts were evaluated using GAPDH primers.

Immunoblot Assays

Whole-cell lysates were prepared in ice-cold RIPA buffer (20 mM Tris, pH 7.4, 137 mM NaCl, 10% glycerol, 0.5% [wt/vol] sodium deoxycholate, 0.1% [wt/vol] sodium dodecyl sulfate (SDS), 1% Triton X-100, 2 mM EDTA) containing 1 mM phenylmethylsulfonyl fluoride and protease inhibitor cocktail (Sigma) and fractionated by SDS–polyacrylamide gel electrophoresis. Primary antibodies against the following proteins were used: VEGF-C (C-20; Santa Cruz), LEDGF/p75 (C16; Santa Cruz), and β-tubulin (Santa Cruz). HRP-conjugated antirabbit secondary antibodies (Jackson ImmunoResearch Laboratories, West Grove, PA) were applied.

In Vivo *Imaging of Tumor Models*

Two different tumor models were used to study blood and lymphatic vasculature. At the end point of the experiment, tumors were fixed (overnight; 4% paraformaldehyde in diethylpyrocarbonate–PBS) and then embedded in paraffin blocks. All the animal experiments were approved by the Weizmann Institutional Animal Care and Use Committee.

In vivo imaging of tumors in dorsal skinfold window chamber model. Window chambers were implanted into the dorsal skinfold of 8-week-old CD-1 nude female mice [40–42]. Briefly, a dorsal skin flap was created and fixed using two metal frames (Research Instruments, Inc, Durham, NC). On one side, a 12-mm circular piece of skin was removed and replaced by a glass cover to enable visual access. Tumors were initiated 48 hours after surgery by injection of 2×10^6 (in 30 μl of PBS) of H1299-DsRed2-IRES (control) or H1299-DsRed2-LEDGF cells to the center of the chamber. Tumor vascular morphology was imaged 4 and 8 days after injection, using the dynamic light scattering imaging (DLSI), which enables imaging of functional blood microvessels using intrinsic signal produced by flow of red blood cells [43,44]. Tumors expressing DsRed were detected by fluorescence microscopy. The imaging setup was composed of a fluorescent zoom stereo microscope SZX12 (Olympus, Japan) coupled with a CCD camera PIXELFLY QE, 12 bit (PCO, Germany), and a laser illumination unit for DLSI (ELFI-C; Elfi-Tech Ltd, Israel).

In vivo imaging of subcutaneous tumors in the mouse ear. Tumors were initiated by intradermal inoculation of C6-DsRed2-IRES (control) or C6-DsRed2-LEDGF (3×10^5 cells in 5 μl of PBS) to the ear of 8-week-old CD-1 nude female mice. Seven days later, high–molecular weight dextran–fluorescein isothiocyanate (FITC, 500 kDa; Sigma) was injected into the ear to enable lymphatic vasculature visualization, using a fluorescent zoom stereo microscope (see section 1). Three channels were collected for each tumor: green fluorescence (dextran-FITC), red fluorescence (tumor DsRed), and DLSI (subjected during processing) for the blood vessels [43,44].

Image Processing and Fractal Analysis

In vivo acquired images were processed using ImageJ (National Institutes of Health; http://rsb.info.nih.gov/ij/). Blood vessels imaged using the DLSI method in the chamber model were traced using "NeuronJ" plug-in (Written by Erik Meijering), producing an image mask.

"Parlance" algorithm images were subjected to fractal analysis to derive the vasculature complexity [45,46]. Briefly, the algorithm covers the image using a set of different-sized boxes. The number of boxes of each size was counted, and its log was plotted against the log of the box length. The positive value of the regression line slope $Df = -S$ was derived, representing the Fractal dimension, which is a quantitative geometric parameter indicative of the complexity (branching and density) of the vascular network. Angiogenesis and lymphangiogenesis would result in higher *Df* values representing higher complexity of the vascular network. *Df* was reported to provide an objective parameter for quantification of expansion of the vascular network in a variety of angiogenesis assays [47–51].

Histologic Analysis

Fixed paraffin-embedded tumor blocks were sectioned serially. The first slide was stained with hematoxylin and eosin, whereas other representative slides underwent immunohistochemical staining and *in situ* hybridization. The immunohistochemical staining sections were deparaffinized with xylene for 5 minutes, followed by sequential ethanol hydration and double-distilled water. Sections were then washed with PBS for 5 minutes and blocked by overnight incubation with 1% BSA in PBS at 4°C. To visualize blood and lymphatic endothelial cells, sections were stained with anti-CD34 (Cedarlane Laboratories, Burlington, NC) or LYVE-1 (Fitzgerald Industries International, Concord, MA) antibodies, respectively.

In Situ *Hybridization*

A specific probe for the *VEGF-C* coding region was prepared by reverse transcription–polymerase chain reaction (RT-PCR) using forward (5′-CTGTGTCCAGCGTAGATGAGC) and reverse (5′-GTAGACGGACACAC ATGGAGG) primers. This probe shares a high degree of homology with both human and mouse complementary DNA (accession nos. NM005429 and NM009506, respectively). Sequence was verified, and the fragment (282 bp) was cloned into the pGEM-T Easy vector system (Promega). Digoxigenin-labeled riboprobes were produced by *in vitro* transcription using a digoxigenin RNA labeling kit (Roche, Basel, Switzerland). Paraffin sections were deparaffinized, and then proteinase K (Sigma) digestion was carried out followed by postfixation in 4% paraformaldehyde in PBS. After two TBS rinses, the sections were dehydrated and air-dried. Slides were then preincubated with hybridization mixture (2× SSC, 10% dextran sulfate, Denhardt solution (Sigma), 50% formamide, and 0.02% SDS) in a humidified oven for 30 minutes at 65°C. Hybridization with the *VEGF-C* probe was initialized by the addition of digoxigenin-labeled antisense or sense riboprobes (1 μg/ml), as well as yeast transfer RNA (100 mg/ml; Sigma). The hybridization procedure was carried out overnight at the previously mentioned conditions. After incubation, slides were rinsed (2 × 10 minutes at room temperature) in 2× SSC containing EDTA (1 mM), once (1 hour, 50°C) in 0.2× SSC containing EDTA, twice (10 minutes at room temperature) in 0.5 × SSC, TBS for (5 minutes at room temperature), and TBS containing BSA (1%; Sigma) for 1 hour at room temperature. The slides were then incubated with anti-digoxigenin alkaline phosphatase (Roche) and were developed using a 5-bromo-4-chloro-3-indolyl-phosphate–nitro blue tetrazolium substrate kit for histochemistry (Roche).

Bioinformatics Analysis

Transcription factor binding site prediction was performed with TFSearch Version 1.3 (http://www.cbrc.jp/research/db/TFSEARCH.html). Genomic analyses were performed at the University of California Santa Cruz (UCSC) genome browser: http://genome.ucsc.edu. The genome builds used were as follows: mouse – mm8; human – hg18; rat – rn4; cow – BosTau2. Tracks used (from the various genomes) include mRNA; Spliced ESTs; ESTs; Human, Mouse, Cow, and Rat Nets; and Conservation.

Statistical Analysis

Data are presented as mean ± SD of at least three independent experiments. Statistical significance ($P < .05$) was assessed by *t* test.

Results

LEDGF/p75 Interacts with VEGF-C

Using *in silico* analysis, five potential LEDGF/p75 binding sites (STRE) were identified in the promoter region of the human *VEGF-C* (chr4:177,950,457–177,950,924, UCSC build hg18; Figure 1*A*, *underline*), two of which were found to be highly conserved between various mammalian species (Figure 1*B*). This finding suggests that LEDGF can potentially bind the VEGF-C promoter and adjust its expression in response to microenvironmental stress. To confirm that LEDGF/p75 binds to these sequences within living cells, a ChIP assay was performed. Indeed, using a specific antibody, LEDGF/p75 was found to bind the *VEGF-C* promoter region, whereas no binding was detected for nonspecific antibodies (Figure 1*C*).

To further test the possible relationship between the LEDGF transcriptional coactivator and the *VEGF-C* gene, we evaluated its effect in human non–small cell lung carcinoma (H1299) cells that have low endogenous expression of VEGF-C. Thus, LEDGF/p75 was overexpressed in the human non–small cell lung carcinoma H1299 cell line, and the levels of VEGF-C mRNA were examined. Transfection was carried out using either an empty expression vector (pIRES) as a control or a construct encoding the rat *LEDGF* gene, tagged with the human influenza virus hemagglutinin (HA) epitope (pIRES-LEDGF). Several puromycin-resistant pools of cells (50 individual clones/pool) along with individual clones were selected, and the expression level of LEDGF/p75 was evaluated by Western blot analysis using anti-HA antibodies (Figure 1*D*). The mRNA levels of LEDGF/p75, VEGF-A, and VEGF-C were examined by RT-PCR in the same pools and clones of cells (Figure 1, *E* and *F*). A notable correlation between the LEDGF/p75 and VEGF-C mRNA levels was detected both in the pool of cells and in the individual clones (regression analysis for all cell lines, $P = .007$; Figure 1, *D–F*). No such correlation was observed between the mRNA levels of VEGF-A and either VEGF-C or LEDGF/p75 (regression analysis of all cell lines, $P = .35$ and .7, respectively; Figure 1, *D–F*).

LEDGF Induces VEGF-C Promoter Activity in a STRE-Dependent Manner

We further investigated the ability of LEDGF/p75 to induce VEGF-C transcription by activation of its promoter; the 468-bp DNA fragment spanning the putative STREs found in the VEGF-C promoter region (Figure 1*A*) was isolated and inserted into a promoter-less luciferase plasmid. In this way, a pVEGF-C-Luc reporter was constructed, enabling detection of the VEGF-C promoter activity. Two additional cell lines with low endogenous expression of VEGF-C, rat glioma C6, and COS7 cells were transiently cotransfected with the pVEGF-C-Luc plasmid together with either a LEDGF/p75–encoding construct (pIRES-LEDGF) or an empty vector (pIRES). Analysis of cell lysates revealed a three-fold induction of the VEGF-C promoter activity in cells expressing LEDGF/p75 compared with control (Figure 2, *A* and *B*). Stable transfection of C6 and H1299 cells with the same constructs resulted in similar results (Figure 2, *C* and *D*).

To determine the importance of the two conserved putative STREs found in the VEGF-C promoter region, several G-to-A substitutions were introduced into these sites (Figure 2*E*). The 468-bp promoter sequence of VEGF-C, bearing the indicated mutations, was then inserted into a promoter-less luciferase plasmid. In the pVEGF-Cm1 plasmid, the function of the proximal putative STRE was disrupted by three mutations. In the pVEGF-Cm2 plasmid, the function of both STREs, as well as one AGG box, was disrupted by nine mutations (Figure 2*E*). H1299 cells were transiently cotransfected with the mutated constructs, together with either a LEDGF/p75–encoding construct (pIRES-LEDGF) or an empty vector (pIRES). Cell lysate analysis indicated that the point mutations introduced within the proximal putative LEDGF/p75 binding site (pVEGF-Cm1-Luc) resulted in a modest 15% loss of the promoter activity compared with the intact promoter construct (pVEGF-Cwt-Luc; Figure 3*F*). However, disruption of both the proximal and the distal STREs (pVEGF-Cm2-Luc) caused a 45% and 68% loss of promoter activity compared with the control either in the absence or in the presence of LEDGF/p75 overexpression, respectively (Figure 2*F*). These data suggest that LEDGF/p75 selectively induces VEGF-C transcription through binding to this conserved STRE sequence found in the promoter region.

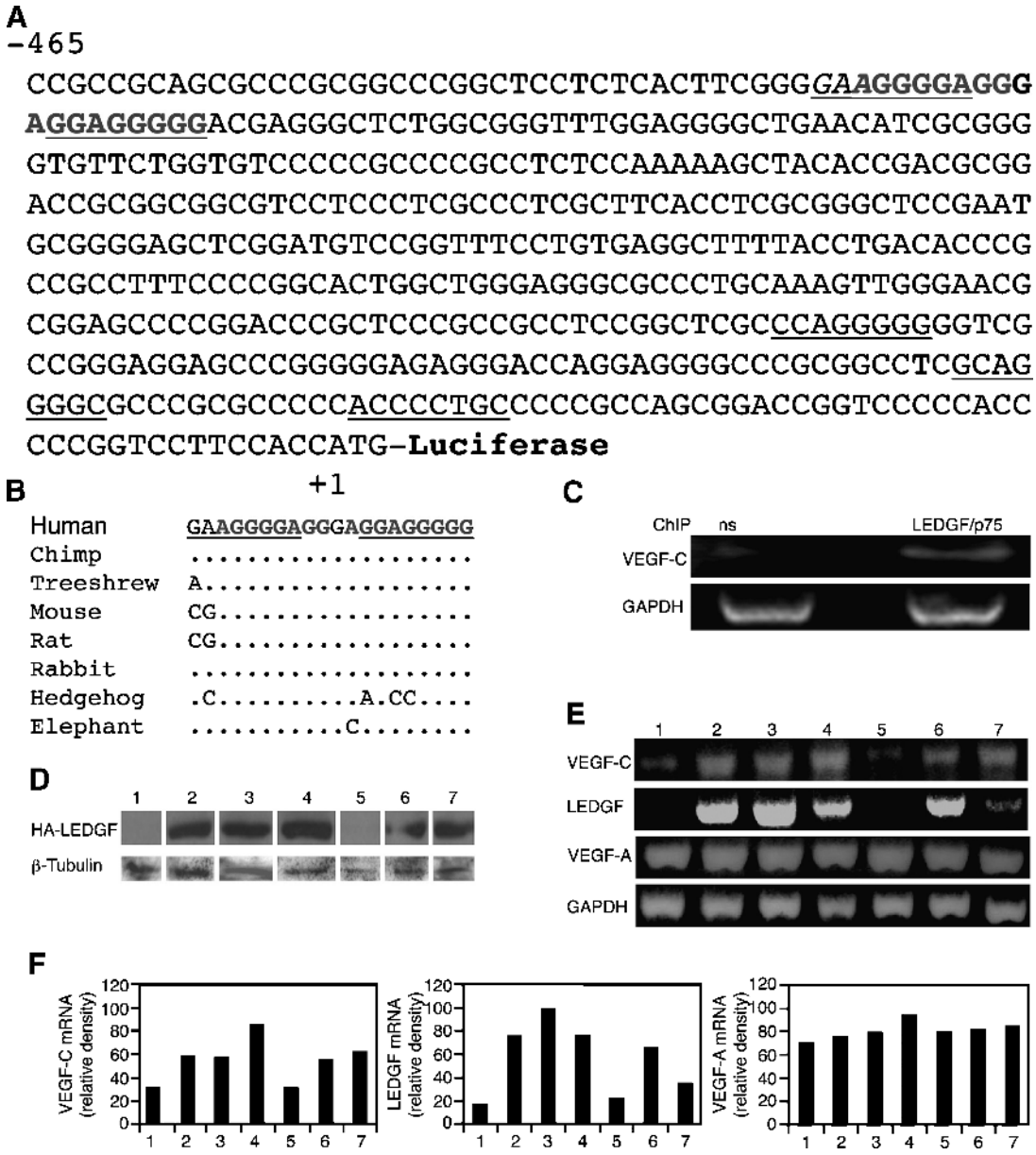

Figure 1. The *VEGF-C* gene contains putative LEDGF/p75 binding sites. (A) Nucleotide sequence of the 468-bp 5′-flanking region of human *VEGF-C* gene. The nucleotide sequences are numbered in relation to the ATG, which is designated "+1". Underlining indicates an STRE, the putative LEDGF binding site. (B) Conservation among species of a putative binding unit for LEDGF was identified using the conservation track of the UCSC genome browser, and the positions of mismatches are indicated. The binding site runs from −426 to −407 (human chr4:177,950,885–177,950,866). (C) ChIP assays were performed using specific primers for the 468-bp VEGF-C promoter (A) and nonspecific antibodies (ns) or anti–LEDGF/p75 antibodies to demonstrate specific binding of LEDGF/p75 in H1299 cells. Evaluation of total genomic DNA was carried out with GAPDH primers. (D) H1299 human lung cancer cells stably transfected either with a control pIRES vector or with a construct encoding rat LEDGF tagged with an influenza virus hemagglutinin epitope (pIRES-HA-LEDGF). Puromycin-resistant pools of cells and individual clones were selected from each of the lines. Immunoblot assay of LEDGF expression levels of puromycin-resistant stably transfected pools (lanes 1 and 2) and individual clones (clones 3-7) using anti–HA antibodies. Protein amounts were quantified using anti–β-tubulin antibodies. (E) RT-PCR analysis of the expression of human VEGF-C, VEGF-A, GAPDH, and transfected rat LEDGF genes was carried out on total RNA extracted from the previously mentioned stably transfected pools and individual clones. (F) Relative densities of the scanned bands normalized against GAPDH.

LEDGF/p75–Induced Expression of VEGF-C Is Activated by Environmental Stress Signals

Previous studies reported that activation of LEDGF/p75 expression by microenvironmental stress results in induced expression of LEDGF/p75 target genes [25,52,53]. Thus, the role of LEDGF/p75 in the regulation of VEGF-C mRNA expression by oxidative stress (0.2 μM H_2O_2), or thermal stress (42°C), was evaluated in H1299 human lung cancer cells (Figure 3). VEGF-C and LEDGF mRNA and protein levels were coinduced under oxidative stress conditions as early as 1 hour; they reached up to 3- and 1.5-fold induction, respectively, after 6 hours of stimulation as determined by RT-PCR (Figure 3, *A* and *B*) and immunoblot using a subunit-specific antibody

directed to the precursor of the human VEGF-C or the p75 variant of LEDGF (Figure 3*C*).

The role of LEDGF/p75 binding sites in the VEGF-C promoter for oxidative and thermal-induced promoter activity was determined by the luciferase assay. H1299 human lung cancer cells were transiently transfected either with intact (pVEGF-Cwt-Luc) or with each one of the two mutated constructs (pVEGF-Cm1-Luc and pVEGF-Cm2-Luc). Subsequently, luciferase activity was measured in cell extracts of H1299 human lung cancer cells subjected to oxidative stress (0.2 μM H_2O_2 for 24 hours). A 10-fold increase of pVEGF-C intact reporter (pVEGF-Cwt-Luc) activity was detected after oxidative stress exposure compared with unstimulated cells (Figure 3*D*). Disruption of the proximal STRE site in pVEGF-Cm1-Luc diminished the promoter activity by 23%, whereas inactivation of both LEDGF/p75 sites in pVEGF-Cm2-Luc abolished 76% of the overall activity (Figure 3*D*). These results were corroborated by ChIP analysis, which demonstrated that the binding of LEDGF/p75 to the *VEGF-C* promoter was significantly enhanced as early as 1 hour after exposure to oxidative stress (Figure 3*E*).

A similar regulation of VEGF-C expression by LEDGF/p75 mRNA was found for thermal stimulation. Thermal stress (42°C for 6 hours) resulted in a two-fold enhancement in VEGF-C mRNA (Figure 3, *F* and *G*) and protein (Figure 3*H*) levels. In addition, thermal stress elicited a two-fold increase in VEGF-C promoter activity, which was reduced by 23% and 73% on disruption of just the proximal (m1) or both proximal and distal (m2) STREs, respectively (Figure 3*I*). As for oxidative stress, ChIP analysis demonstrated enhanced binding of LEDGF/p75 to the VEGF-C promoter as early as 1 hour after exposure to thermal stress (Figure 3*J*).

As further evidence for the role of LEDGF/p75 in mediating stress-induced expression of VEGF-C, both LEDGF/p75 and VEGF-C were significantly induced when H1299 human lung cancer cell cultures were subjected to elevated column of culture medium, resulting in hypoxic condition and slightly elevated hydrostatic pressure (Figure W1). These results indicate that various stress signals enhance the transcriptional activity of *VEGF-C* gene in a LEDGF/p75 (and STRE)–dependent manner.

LEDGF cis-*Native Antisense Transcript and siRNA Diminish VEGF-C mRNA Expression*

A search of the LEDGF/p75 locus in the mRNA track of the mouse genome database (UCSC genome browser [54], genome build mm8; Figure 4*A*) identified a few complementary DNA oriented in a direction consistent with their transcription from the opposite strand of the *LEDGF* locus, representing putative *cis*-encoded natural antisense mRNA of LEDGF. One of the putative *cis*-encoded natural antisense transcripts (*cis*-NATs), AK042735, was specific to the p75 variant of LEDGF. AK042735 is a 3184-bp-long single-exon transcript and does not seem to encode for a protein. It overlaps exons 11 to 14 of LEDGF/p75 on the opposite strand (Figure 4*B*) and is in complete overlap with the LEDGF/p75 locus [55]. Additional database searches identified similar EST clone sequences within the rat and cow EST databases (genome builds rn4 and BosTau2, respectively; Figure 4*C*). Furthermore, in the human database, two discontinuous ESTs were discovered *in silico* (genome build hg18), which were found, by RT-PCR and DNA sequence analyses, to be contiguous mRNA (Figure 4, *C* and *D*). Similarly, the existence of mouse and rat putative *cis*-NATs was verified

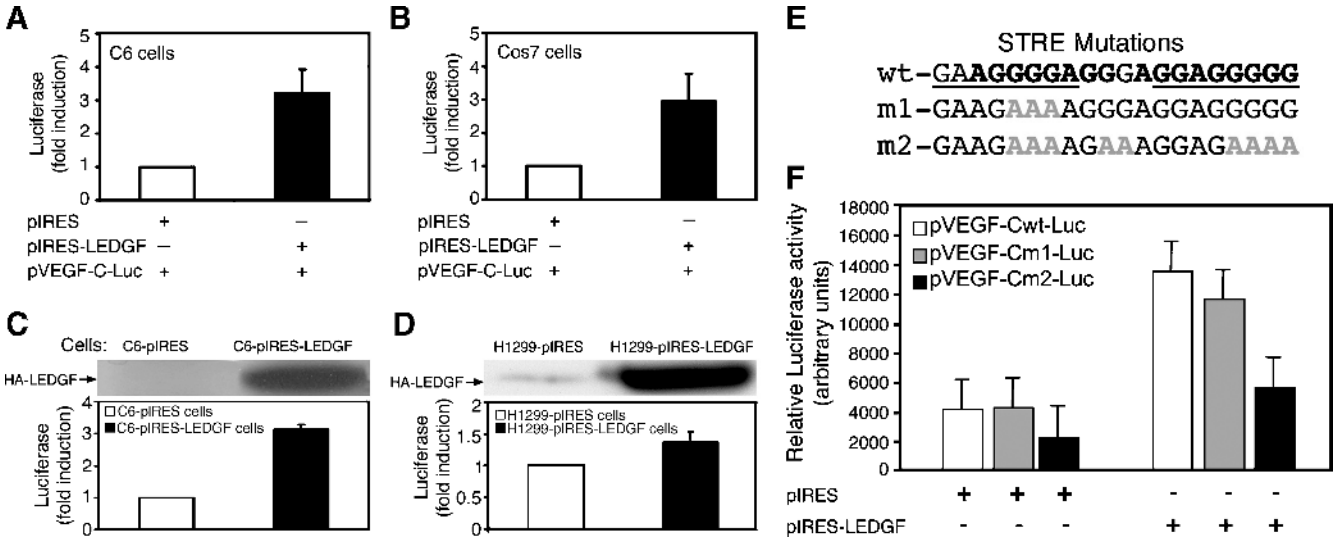

Figure 2. LEDGF/p75 transcriptionally activates VEGF-C expression in an STRE-dependent manner. A luciferase reporter gene containing the 5′-flanking region of human *VEGF-C* gene (Figure 1*A*, pVEGF-C-Luc) was transiently cotransfected with a control empty vector (pIRES) or with a construct encoding LEDGF/p75 into rat glioma C6 or COS7 cells (A and B, respectively). Luciferase activity under each experimental condition was scaled relative to the activity in control cells (mean ± SD, $n = 3$). (C and D; upper panel) Western blot analysis carried out using anti–HA antibodies of protein extracted from C6 rat glioma (C) or human H1299 (D) cells stably expressing the rat LEDGF protein tagged to hemagglutinin (HA) epitope (pIRES-LEDGF) after selection with puromycin. (C and D; lower panel) Measurement of luciferase activity in C6 (C) or H2299 (D) cells stably expressing either LEDGF protein (pIRES-LEDGF) or the empty control vector (pIRES) transiently transfected with the pVEGF-C-Luc construct. (E) Wild type (wt) and two mutated (m1 and m2) sequences of the conserved LEDGF/p75 binding sites are presented, and the G-to-A substitutions are indicated in gray. (F) H1299 cells were transiently cotransfected either with intact pVEGF-Cwt-Luc reporter or pVEGF-Cm1-Luc, pVEGF-Cm2-Luc together with LEDGF/p75 expression vector or a control empty vector (+ and − indicate presence and absence of each construct; mean ± SD, $n = 3$).

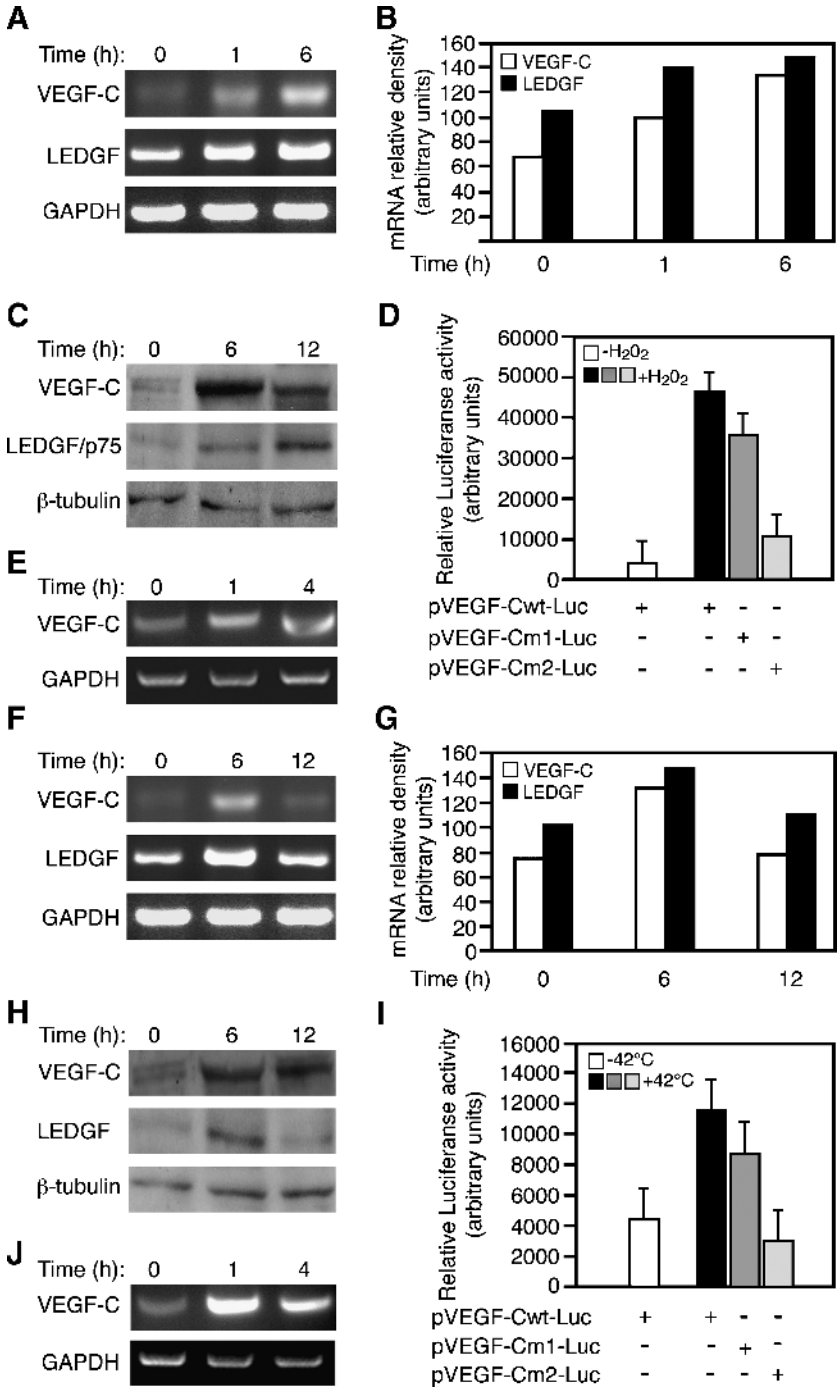

Figure 3. VEGF-C expression is induced by environmental stress. (A) VEGF-C and LEDGF-p75 mRNA expression was analyzed by RT-PCR analysis in H1299 human lung cancer cells exposed for 1 and 6 hours to 0.2 mM H_2O_2 relative to untreated cells. (B) Relative intensity of the bands normalized against GAPDH. (C) Immunoblot assay of VEGF-C, LEDGF, and β-tubulin in H1299 cells treated with 0.2 mM H_2O_2 for 6 or 12 hours or left untreated. (D) Luciferase reporter assay was used with a construct composed of a 468-bp *VEGF-C* wild-type gene fragment (pVEGF-Cwt-Luc) or mutation constructs carrying G-to-A substitutions in the LEDGF/p75 binding sites (pVEGF-Cm1-Luc and pVEGF-Cm2-Luc). H1299 cells transfected with the previously mentioned reporters were stimulated 24 hours after transfection with 0.2 mM H_2O_2 or were left untreated (mean ± SD, $n = 3$). (E) LEDGF binding to *VEGF-C* gene sequences was analyzed by ChIP. Chromatin from cells that were exposed to 0.2 mM H_2O_2 for 1 and 4 hours or left untreated (0 hour) was immunoprecipitated (ChIP) with anti–LEDGF/p75–specific antibody and analyzed by PCR using primers spanning the 468-bp *VEGF-C* promoter (Figure 1*A*). Evaluation of total genomic DNA was carried out with GAPDH primers. (F) VEGF-C and LEDGF/p75 mRNA expression was analyzed by RT-PCR analysis either in H1299 lung cancer cells grown at 42°C for 6 hours, transferred for an additional 6-hour incubation at 37°C (12 hours) or left at 37°C (0 hour). (G) Relative intensity of the bands normalized to GAPDH. (H) Immunoblot assay of VEGF-C, LEDGF, and β-tubulin in H1299 cells treated as indicated in panel F. (I) Luciferase reporter assay carried out with pVEGF-Cwt-Luc or two mutated constructs pVEGF-Cm1-Luc and pVEGF-Cm2-Luc. H1299 cells transfected with the previously mentioned reporters were heat-activated (42°C) for 6 hours and then maintained for an additional 6 hours at 37°C (+ and − indicate presence and absence of each construct, respectively; mean ± SD $n = 3$). (J) ChIP analysis as was described in panel E, except that cells were heat-activated (42°C) for the indicated time.

by RT-PCR (Figure 4*D*), and the fidelity of the products was confirmed by DNA sequence analysis.

To investigate the biologic activities of LEDGF/p75 *cis*-NAT and its significance with respect to the regulation of VEGF-C mRNA and protein levels, the human *cis*-NAT (LEDGFas) was inserted into the pIRES plasmid vector (pIRES-LEDGFas) and used to transfect human lung A549 cells to generate stable transfectants. A pool of clones was selected by puromycin, and the expression level of LEDGFas was found to increase by two-fold compared with cells transfected with an empty vector (Figure 4, *E* and *F*). The expression of LEDGFas reduced LEDGF/p75 sense mRNA by only 15% but strongly reduced VEGF-C mRNA levels (46%; Figure 4, *E* and *F*). Moreover, the expression of LEDGFas resulted in a robust reduction in protein levels of both LEDGF/p75 and VEGF-C (Figure 4*G*).

The ability of LEDGFas to interfere with stress-induced transcriptional activation of the VEGF-C promoter was tested in H1299 human lung cancer cells transiently cotransfected with pVEGF-C-Luc construct together with either a construct encoding the LEDGF/p75 antisense transcript or an empty pIRES vector. Cells were subjected either to oxidative (0.2 mM H_2O_2 for 24 hours) or thermal (42°C for 6 hours)

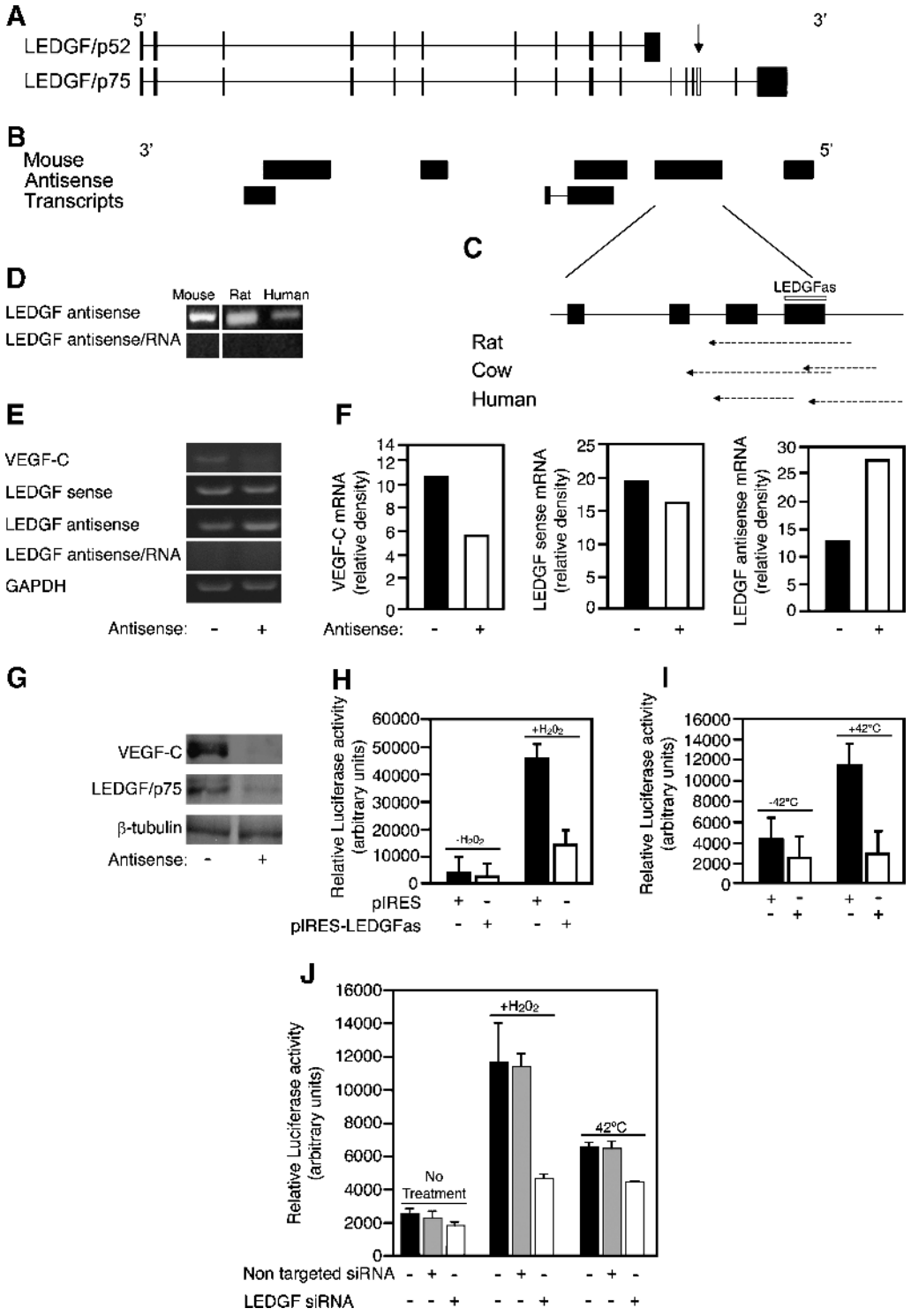

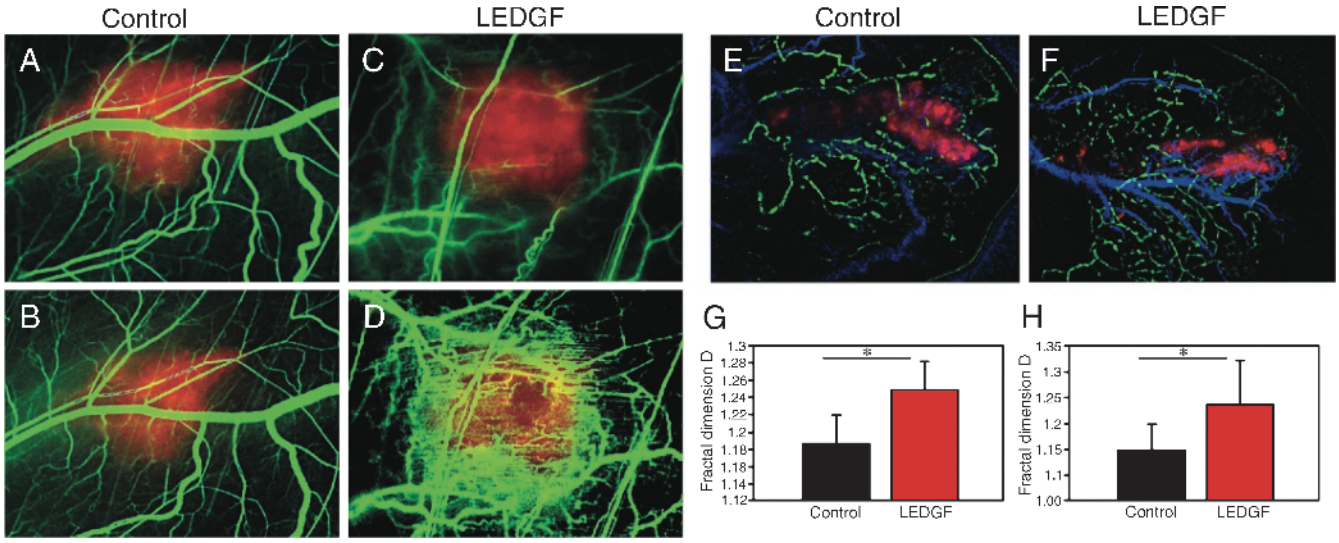

Figure 5. LEDGF-induced remodeling of blood and lymph vessels network. *In vivo* imaging of H1299 tumors developed in skinfold window chamber (A–D, G). (A–D) Overlay of tumor fluorescence (red) and blood vessels processed using DLSI image (green). Tumors were initiated in the CD-1 nude mice by injecting subcutaneously into a window chamber H1299 cells cotransfected with DsRed and either a control or an LEDGF-encoding plasmid (C, D). Tumor development was followed and imaged 4 (B) and 8 (D) days after tumor cell inoculation. Graph (G) indicates a mean fractal dimension value – *D*, calculated by fractal box count method [45], represents the complexity of the blood vessels' network. Blood vessels' network induced by the LEDGF-overexpressing tumors is significantly more complex ($P = .025$). *In vivo* imaging of C6 tumors developed in the edge of mouse ear (E, F, and H). Overlay of tumor fluorescence (red), blood vessels' DLSI image, and lymph vessels network (green). Tumors were initiated in CD-1 nude mice by injection of C6 cells cotransfected with DsRed and either a control (E) or an LEDGF-encoding plasmid (F). Tumor vasculature was imaged 7 days after cell inoculation. Complexity analysis of the lymphatic network (H) shows the overexpression of LEDGF results in significantly ($P = .0194$) more complex network.

stress. Both basal and stress-induced promoter activities were significantly attenuated by the presence of LEDGFas expression (Figure 4, *H* and *I*).

The role of LEDGF/p75 in basal and stress-induced expressions of VEGF-C were further highlighted by the ability to attenuate the baseline expression of VEGF-C and substantially suppress stress-induced expression of VEGF-C using siRNA targeting LEDGF/p75 (Figure 4*J*). H1299 cells showed a significant 21% attenuation of VEGF-C promoter activity by knockdown of LEDGF/p75 expression relative to cells treated with nontargeted siRNA or control cells ($P < .05$; 1-tailed *t* test). Robust activation of VEGF-C promoter expression was observed by H_2O_2 and hyperthermia in untreated cells as well as cells transfected with nonspecific siRNA ($P < 2 \times 10^{-6}$; 2-tailed *t* test). Knockdown of LEDGF/p75 attenuated the activity of VEGF-C promoter by 60% for H_2O_2 and by 32% for hyperthermia ($P < .001$; 2-tailed *t* test; relative to control cells and cells treated with nonspecific siRNA subjected to the respective stress).

These results confirm that LEDGF mediates VEGF-C activity and that targeting its expression can be used to suppress VEGF-C in tumors. Moreover, we showed here the activity of the LEDGF/p75 *cis*-NAT, suggesting that it may have an important role in physiological regulation of VEGF-C expression.

Figure 4. Attenuation of VEGF-C expression by *cis*-natural antisense RNA of LEDGF/p75 and by LEDGF/p75 siRNA. (A) Illustration of the genomic structure of LEDGF variants. Black boxes indicate exons, and the connecting line indicates introns. The representative sequences shown are AF339083 (LEDGF/p52) and NM_133948.4 (LEDGF/p75). (B) Diagram of the mouse *cis*-NATs. Accession numbers are as follows (in order of start position from left to right): AK140469, AK038357, AK020824, AK171985, AK053153, AK042735, and AK143096. (C) Expansion of the genomic region covered by the *cis*-NAT AK042735. The 214-bp-long exon probe that was designed against the *cis*-NAT of LEDGF is indicated by an empty box. Accession numbers of equivalent transcripts in other species: rat – CB576984; human – AV716383, DA171947; cow – CK778664, BF654277. (D) RT-PCR analysis of RNA from mouse, rat, and human origins performed with LEDGF/p75 antisense-specific primers designed to encompass the exon probe (indicated by an open box 4 in panels A and C and an arrow in panel A). Row antisense/RNA indicates that RT reaction was carried out with no enzyme supplementation and serves as a control to monitor genomic contamination in the samples. (E) Analysis of VEGF-C and LEDGF sense and antisense transcripts by specific RT-PCR in control A549 (−) or stably overexpressing LEDGF antisense construct (+). For amplification of antisense transcripts, sense-specific primers were added to reverse transcription, whereas for the detection of the sense transcripts, antisense primers were added to reverse transcription. Row antisense/RNA is as in panel D. (F) Relative intensity of the bands was normalized against GAPDH and is summarized in the bar graph. (G) Immunoblot assay of VEGF-C, LEDGF/p75, and β-tubulin protein extracted from A549 cells stably transfected with an empty vector (−) or with a construct expressing LEDGF antisense (+). (H and I) H1299 cells were cotransfected with *VEGF-C*–luciferase reporter and empty vector (pIRES) or vector expressing LEDGF antisense (pIRES-LEDGFas) that reduces the expression of LEDGF/p75. Cells were then incubated with 0.2 mM H_2O_2 for 12 hours (H) or heated to 42°C for 6 hours followed by an additional 6-hour incubation at 37°C (I; mean ± SD, $n = 3$). (J) Attenuation of pVEGF-Cwt-Luc reporter activity as a result of knockdown of LEDGF/p75 expression using a specific synthetic siRNA. As a control, a nontarget siRNA was applied (mean ± SD, $n = 3$).

Ectopic Expression of LEDGF Promoted Tumor Angiogenesis and Lymphangiogenesis and Induced VEGF-C Expression

To evaluate whether enhanced expression of LEDGF/p75 was sufficient for stimulating the expansion of subcutaneous blood and lymphatic vessels, subcutaneous angiogenesis and lymphangiogenesis were assessed by intravital imaging using two tumor models, a dorsal skinfold window chamber and subcutaneous tumors in the mouse ear. H1299 human lung cancer cells and C6 rat glioma cells, both of which express a low endogenous level of VEGF-C, were engineered to stably express DsRed2 fluorescent protein alone (control) or together with LEDGF. Tumors were established in 8-week-old CD-1 nude female mice (n = 5 per group) by inoculating either a suspension of fluorescent H1299 cells (2×10^6) to the center of a dorsal skinfold window chamber or C6 cells (3×10^5) to the edge of the mouse ear.

Functional blood vessels were visualized by DLSI (*green*) [43,44], whereas the tumor signal was detected by fluorescence microscopy (*red*; Figure 5, *A–D*). A significant increase in functional blood vessel density was detected in LEDGF-overexpressing H1299 tumors developed within the dorsal skinfold window chamber as early as 8 days after tumor cell inoculation (Figure 5, *C* and *D*) in comparison to control tumors (Figure 5, *A* and *B*). The tumor blood vasculature in each group of mice (n = 5) was analyzed using the fractal box count method, providing the complexity of blood vessel network. A significant increase (P = .025) in blood vessels' complexity was deduced from the analysis of LEDGF-overexpressing tumors in comparison to control tumors (Figure 5*E*).

The lymphatic network was visualized 7 days after inoculation of C6 glioma cells to the mouse ear by intradermal injection of dextran-FITC (500 kDa; green) in two sites of a mouse ear, whereas the tumor was detected by fluorescence microscopy (*red*) and blood vessels were detected by DLSI (*blue*; Figure 5, *E* and *F*). A pronounced elevation in lymphatic network complexity was induced by the LEDGF-expressing tumors, showing increased density in comparison to control tumors (Figure 5, *E* and *F*). Further fractal box-count analysis of the lymphatic network revealed that overexpression of LEDGF results in a significantly more complex network (Figure 5*H*; P = .0194).

The impact of LEDGF/p75 overexpression was evaluated in histologic specimens generated from the previously mentioned tumors at the end point of each experiment. No significant pathologic differences were observed by hematoxylin-eosin histologic sections of the unifocal tumors developed in the dorsal skinfold window chamber in the presence or absence of LEDGF overexpression (Figure 6, compare *A*

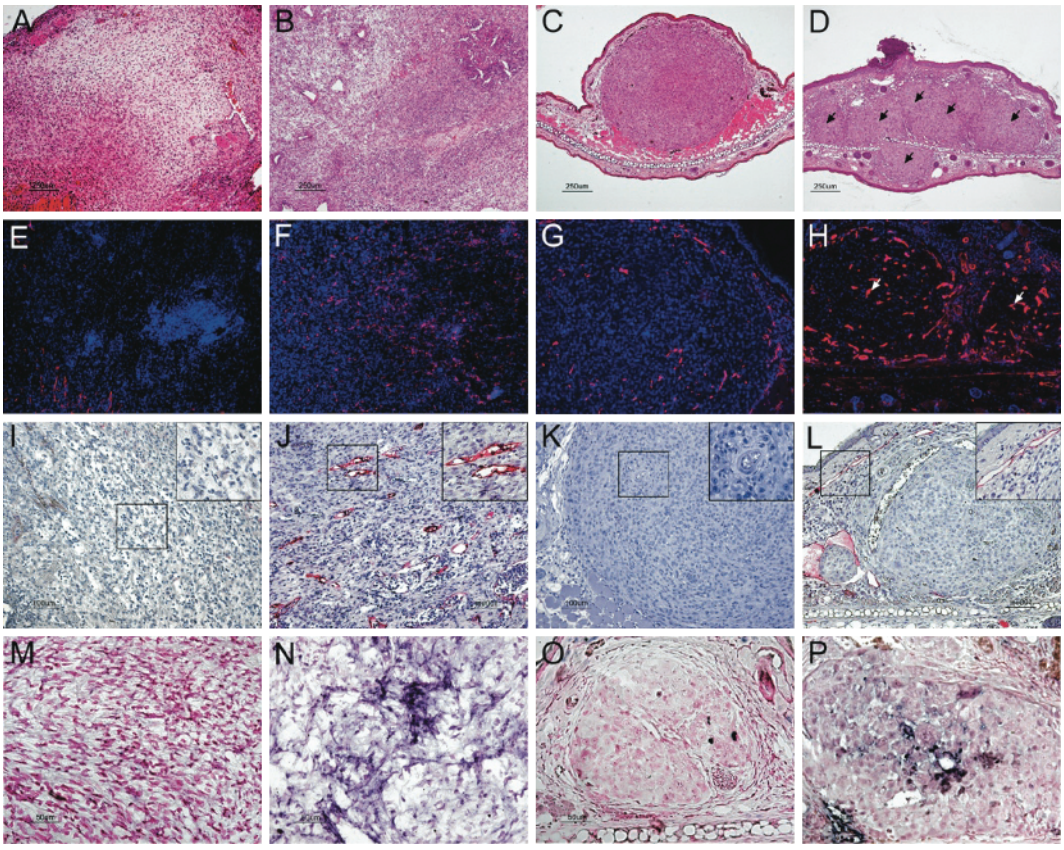

Figure 6. LEDGF/p75 overexpression in tumors stimulates blood and lymphatic vessels' sprouting and induction of VEGF-C expression. *Ex vivo* analysis of subcutaneous tumors excised from mice inoculated with tumor cells in a dorsal skinfold window chamber (H1299 cells; A, B, E, F, I, J, M, and N) or in a tip of an ear (C6 cells; C, D, G, H, K, L, O, and P). Histologic sections stained with hematoxylin-eosin. (A and B) H1299 control and LEDGF-overexpressing tumors, respectively. (C and D) C6 control and LEDGF-overexpressing tumors. Scale bar, 200 μm. Immunohistochemical staining with anti-CD34 antibody of blood vessels in control H1299 and C6 (E and F, respectively) and LEDGF-overexpressing tumors (G and H, respectively; scale bar, 100 μm). Immunohistochemical staining of lymphatic endothelial cells using anti–LYVE-1 antibodies (H1299: control [I] and LEDGF-overexpressing tumors [J]; C6: control [K] and LEDGF-overexpressing tumors [L]; scale bar, 100 and 50 μm in the insert picture). *In situ* hybridization analysis using VEGF-C as a probe, indicating that VEGF-C expression is induced in tumors initiated from cells overexpressing LEDGF (H1299: control [M] and LEDGF overexpression [N]; C6: control [O] and LEDGF overexpression [P]; scale bar, 100 μm).

with *B*). In contrast, in the ear tumor model, overexpression of LEDGF developed multifocal tumors along the entire peripheral side of the ear (Figure 6, *arrows*), whereas control cells developed a single tumor (Figure 6, compare *C* with *D*). The effects on the tumor growth pattern are in accord with the effect of LEDGF on cell invasion and migration (Figure W2).

Blood vessel density was elevated by LEDGF overexpression in the two tumor models, as determined through immunohistochemical staining using a MoAb against CD34 (Figures 6 and W3). However, the effect of LEDGF on the density of vessels was statistically significant only for H1299 tumors, in which the baseline vessel density was lower relatively to the highly angiogenic C6 tumors (Figures 6, *G*, *H*, and *E*, *F*, and W3; 3.97-fold, $P = .07$; and 3.26-fold, $P = .01$; increased vessel count for C6 and H1299, respectively). Conversely, LYVE-1, a lymphatic endothelial marker, revealed that overexpression of LEDGF/p75 significantly increased the density of lymphatic vessels within and around tumors for both C6 and H1299 tumors (Figures 6, *I*, *J* and *K*, *L*, and W3; 56.39-fold, $P = 1.2 \times 10^{-6}$; and 3.43-fold, $P = .02$; increased density of LYVE-1–positive vessels for C6 and H1299, respectively).

In situ hybridization analysis demonstrated enhanced VEGF-C expression in H1299-LEDGF, as well as in C6-LEDGF tumors (Figure 6, *M*, *N* and *O*, *P*, respectively), which was consistent with the prominent LEDGF overexpression level. Thus, the *in vivo* analysis of tumor xenografts in the two distinct models corroborated the role of LEDGF in inducing the expression of VEGF-C and regulating angiogenesis and lymphangiogenesis in tumors.

Discussion

Angiogenesis and lymphangiogenesis provide complementary mechanisms for matching tissue requirements for nutrient supply and waste product clearance. Thus, regulation of both processes should be fine-tuned to microenvironmental signals. A notable example is the regulation of angiogenesis by the hypoxia-induced expression of VEGF-A, as mediated by the activity of hypoxia-inducible factor 1 [56]. We report here an analogous molecular pathway modulating lymphangiogenesis through the stress-regulated expression of VEGF-C mediated by LEDGF/p75 (Figure W4).

VEGF-C is currently considered to play a central role in the control of lymphatic endothelial cell biology during embryogenesis [3], tumorigenesis [57], and metastasis [58]. The study presented here reports the identification of a novel molecular mechanism for microenvironmental regulation of VEGF-C activity. We demonstrated that VEGF-C expression is controlled *in vitro* and *in vivo* by the p75 splice variant of LEDGF, a novel growth and survival transcriptional activator. VEGF-C can thus be added to a growing list of stress-related proteins, including antioxidant protein 2, Hsp27, αB-crystallin, and Hsp90, all of which are transcriptionally regulated by LEDGF/p75 [29,59].

LEDGF activity is induced by a variety of environmental stress signals and regulates downstream response pathways by enhancing expression through binding to a specific STRE and/or HSE consensus core sequence, located in the promoter region of its target genes. It was shown here that LEDGF/p75 transactivated VEGF-C transcription by interacting with specific species-conserved STREs. Disruption of these conserved STREs significantly attenuated the expression of VEGF-C. Point mutations introduced within these conserved STREs suppressed the transcription activity of the *VEGF-C* gene.

In addition to its role as a survival factor, LEDGF/p75 was implicated in various human diseases including atopic disorders [31], integration of the human immunodeficiency virus in acquired immunodeficiency syndrome [60], and cancer. It was shown to be involved in a t(9;11)(p22;p15) recurrent translocation to form a NUP98-LEDGF fusion protein in acute and chronic myeloid leukemia [61]. LEDGF was recently found to be associated with MLL and menin, thus placing it at the center of a pathway in cancer pathogenesis [62]. LEDGF/p75 expression is elevated in 93% of prostate tumors [32]. It was reported that αB-crystallin, a target of LEDGF, is expressed in basal-like tumors and predicted poor survival in breast cancer patients [63].

An additional target of LEDGF, heat shock protein 27 (Hsp27), is highly expressed in tumors and contributes to tumor progression and metastasis [26]. Moreover, LEDGF/p75 was shown to be associated with JPO2, a Myc-binding protein [64]. LEDGF/p75 was also reported to control a caspase-independent lysosomal cell death pathway in cancer cells [33]. Thus, LEDGF/p75 seems to be implicated in multiple pathways affecting cancer progression. It also has an important role during development, as was evident by the perinatal lethality of LEDGF-deficient mice [65].

As shown here, VEGF-C expression was induced by LEDGF/p75 overexpression, whereas suppression of cellular LEDGF using a synthetic LEDGF antisense construct, attenuated the endogenous VEGF-C mRNA and polypeptide levels. To evaluate whether elevated expression of LEDGF/p75 was sufficient for induction of angiogenesis and lymphangiogenesis, we challenged the subcutaneous vasculature to H1299 human lung cancer cells and C6 rat glioma cells engineered to overexpress LEDGF/p75. Both cell lines were found to express low endogenous level of both VEGF-C and LEDGF/p75, and expression was augmented by elevated expression of LEDGF/p75. Intravital microscopy revealed increased density of subcutaneous blood vessels in the periphery of LEDGF/p75–overexpressing H1299 tumors and increased density of lymphatic vessels in the periphery of LEDGF/p75–overexpressing C6 tumors. Quantitative analysis of both vascular beds was done by semiautomatic determination of the fractal dimension *Df* [47–51].

Accordingly, histologic analysis showed that ectopic overexpression of LEDGF/p75 was sufficient for promoting tumor VEGF-C expression, angiogenesis, and lymphangiogenesis. Lymphangiogenesis was significantly and robustly induced, resulting in increased density of LYVE-1–positive lymphatic vessels for both C6 and H1299 tumors. Histologic sections revealed a significantly elevated density of CD34-positive blood vessels for both tumor types; however, the change was statistically significant only for H1299 tumors in which the endogenous density of blood vessels was low relative to the highly angiogenic C6 tumors.

The observation that subcutaneous LEDGF-overexpressing C6 cells generated multifocal tumors may indicate that these cells inherited both migration and invasion potential, as shown previously for VEGF-C–overexpressing cells, using this tumor model [8]. As shown here, LEDGF/p75–induced migration and invasion could be measured *in vitro* also for H1299 cells. These tumorigenic properties may further explain the observed aggressiveness of tumors that express high LEDGF/p75 levels.

Future studies should evaluate the significance of LEDGF/p75 in the regulation of expression of VEGF-C in human cancers. The impact of overexpression of LEDGF/p75 on tumor angiogenesis, lymphangiogenesis, invasion, and migration suggests that it could affect progression also for tumors with low propensity to form lymph node metastases. Moreover, VEGF-C induced by LEDGF/p75 could potentially help sustain tumor progression in a VEGF-A refractory manner, providing tumors with a potential mechanism to escape VEGF-A–targeted therapy. The clinical significance of this pathway remains to be evaluated.

An interesting aspect is the regulation of LEDGF by reactive oxygen species (ROS) in general and by hydrogen peroxide (H_2O_2) in particular. Increased levels of H_2O_2 were linked to DNA alterations, cell proliferation, apoptosis resistance, metastasis, and angiogenesis in cancer [66,67]. We reported here that VEGF-C expression is significantly stimulated in the presence of H_2O_2 in a LEDGF/p75–dependent manner. Similarly, hyperthermia the expression of both LEDGF/p75 and VEGF-C. Previously, it was reported that cells subjected to a transient 4-hour exposure to 42°C followed by a 24-hour recovery showed suppressed expression of VEGF-A and reduced angiogenesis [68]. Thus, hyperthermia can possibly augment angiogenesis and lymphangiogenesis by the elevated expression of LEDGF/p75 and VEGF-C, whereas resolution of hyperthermia-induced angiogenesis and recovery from hyperthermic stress is associated with the attenuated expression of VEGF-A.

The regulation of LEDGF expression may help shed light on the stress response pathways in tumor cells. *In silico* data supported the existence of *cis*-NAT of mouse, human, rat, and cow LEDGFas, which are transcribed from the opposite strand of the *LEDGF* locus and are specific for the p75 variant. Natural antisense RNA are widely distributed to viruses, prokaryotes, and eukaryotes and are also predicted to be abundant in mammals, including both human and mouse [69]. Indeed, computer predictions have estimated that natural antisense genes comprise as much as 20% of the human genome [70]. Antisense RNA may contribute to regulatory activity at various levels, such as posttranscription, splicing, transport, and genomic imprinting [71]. We demonstrated that the human *cis*-natural antisense mRNA of LEDGF was functionally active and was able to regulate *in vitro* both basal and stress (H_2O_2 and heat shock)–induced VEGF-C levels. Ectopic expression of LEDGFas significantly diminished LEDGF/p75 protein amounts, whereas its effect on RNA level was less prominent. Thus, we hypothesize that LEDGFas represents a novel posttranscriptional gene regulation layer that specifically controls LEDGF/p75 polypeptide levels and LEDGF/p75 functions.

In summary, we report here a novel role for LEDGF/p75 in controlling microenvironmental regulation of structural changes in the lymphatic vasculature through expression of VEGF-C. Lymphangiogenesis, induced in response to stress cues, can alleviate edema and help maintain tissue homeostasis by augmenting the capacity for fluid clearance but can also facilitate tumor metastasis. The effect of LEDGF/p75 on tumor expression of VEGF-C and lymphangiogenesis suggests that LEDGF/p75 should be evaluated among the multiple potential targets for cancer therapy.

Acknowledgments

The authors thank Calanit Raanan and the late Dorit Natan for preparations of histologic sections and Haya Avital and Amit Mishali for the artwork.

References

[1] Joukov V, Sorsa T, Kumar V, Jeltsch M, Claesson-Welsh L, Cao Y, Saksela O, Kalkkinen N, and Alitalo K (1997). Proteolytic processing regulates receptor specificity and activity of VEGF-C. *EMBO J* **16**, 3898–3911.

[2] Saaristo A, Veikkola T, Enholm B, Hytonen M, Arola J, Pajusola K, Turunen P, Jeltsch M, Karkkainen MJ, Kerjaschki D, et al. (2002). Adenoviral VEGF-C overexpression induces blood vessel enlargement, tortuosity, and leakiness but no sprouting angiogenesis in the skin or mucous membranes. *FASEB J* **16**, 1041–1049.

[3] Karkkainen MJ, Haiko P, Sainio K, Partanen J, Taipale J, Petrova TV, Jeltsch M, Jackson DG, Talikka M, Rauvala H, et al. (2004). Vascular endothelial growth factor C is required for sprouting of the first lymphatic vessels from embryonic veins. *Nat Immunol* **5**, 74–80.

[4] He Y, Rajantie I, Pajusola K, Jeltsch M, Holopainen T, Yla-Herttuala S, Harding T, Jooss K, Takahashi T, and Alitalo K (2005). Vascular endothelial cell growth factor receptor 3–mediated activation of lymphatic endothelium is crucial for tumor cell entry and spread via lymphatic vessels. *Cancer Res* **65**, 4739–4746.

[5] Skobe M, Hawighorst T, Jackson DG, Prevo R, Janes L, Velasco P, Riccardi L, Alitalo K, Claffey K, and Detmar M (2001). Induction of tumor lymphangiogenesis by VEGF-C promotes breast cancer metastasis. *Nat Med* **7**, 192–198.

[6] Mattila MM, Ruohola JK, Karpanen T, Jackson DG, Alitalo K, and Harkonen PL (2002). VEGF-C induced lymphangiogenesis is associated with lymph node metastasis in orthotopic MCF-7 tumors. *Int J Cancer* **98**, 946–951.

[7] Karpanen T, Egeblad M, Karkkainen MJ, Kubo H, Yla-Herttuala S, Jaattela M, and Alitalo K (2001). Vascular endothelial growth factor C promotes tumor lymphangiogenesis and intralymphatic tumor growth. *Cancer Res* **61**, 1786–1790.

[8] Hoshida T, Isaka N, Hagendoorn J, di Tomaso E, Chen YL, Pytowski B, Fukumura D, Padera TP, and Jain RK (2006). Imaging steps of lymphatic metastasis reveals that vascular endothelial growth factor-C increases metastasis by increasing delivery of cancer cells to lymph nodes: therapeutic implications. *Cancer Res* **66**, 8065–8075.

[9] Mandriota SJ, Jussila L, Jeltsch M, Compagni A, Baetens D, Prevo R, Banerji S, Huarte J, Montesano R, Jackson DG, et al. (2001). Vascular endothelial growth factor-C mediated lymphangiogenesis promotes tumour metastasis. *EMBO J* **20**, 672–682.

[10] Cueni LN and Detmar M (2008). The lymphatic system in health and disease. *Lymphat Res Biol* **6**, 109–122.

[11] Saaristo A, Karpanen T, and Alitalo K (2000). Mechanisms of angiogenesis and their use in the inhibition of tumor growth and metastasis. *Oncogene* **19**, 6122–6129.

[12] Burton JB, Priceman SJ, Sung JL, Brakenhielm E, An DS, Pytowski B, Alitalo K, and Wu L (2008). Suppression of prostate cancer nodal and systemic metastasis by blockade of the lymphangiogenic axis. *Cancer Res* **68**, 7828–7837.

[13] Shibata MA, Morimoto J, Shibata E, and Otsuki Y (2008). Combination therapy with short interfering RNA vectors against VEGF-C and VEGF-A suppresses lymph node and lung metastasis in a mouse immunocompetent mammary cancer model. *Cancer Gene Ther* **15**, 776–786.

[14] Leak LV (1976). The structure of lymphatic capillaries in lymph formation. *Fed Proc* **35**, 1863–1871.

[15] Dafni H, Cohen B, Ziv K, Israely T, Goldshmidt O, Nevo N, Harmelin A, Vlodavsky I, and Neeman M (2005). The role of heparanase in lymph node metastatic dissemination: dynamic contrast-enhanced MRI of Eb lymphoma in mice. *Neoplasia* **7**, 224–233.

[16] Dafni H, Gilead A, Nevo N, Eilam R, Harmelin A, and Neeman M (2003). Modulation of the pharmacokinetics of macromolecular contrast material by avidin chase: MRI, optical, and inductively coupled plasma mass spectrometry tracking of triply labeled albumin. *Magn Reson Med* **50**, 904–914.

[17] Dafni H, Israely T, Bhujwalla ZM, Benjamin LE, and Neeman M (2002). Overexpression of vascular endothelial growth factor 165 drives peritumor interstitial convection and induces lymphatic drain: magnetic resonance imaging, confocal microscopy, and histological tracking of triple-labeled albumin. *Cancer Res* **62**, 6731–6739.

[18] Goldman J, Conley KA, Raehl A, Bondy DM, Pytowski B, Swartz MA, Rutkowski JM, Jaroch DB, and Ongstad EL (2007). Regulation of lymphatic capillary regeneration by interstitial flow in skin. *Am J Physiol* **292**, H2176–H2183.

[19] Boardman KC and Swartz MA (2003). Interstitial flow as a guide for lymphangiogenesis. *Circ Res* **92**, 801–808.

[20] Rutkowski JM, Moya M, Johannes J, Goldman J, and Swartz MA (2006). Secondary lymphedema in the mouse tail: lymphatic hyperplasia, VEGF-C upregulation, and the protective role of MMP-9. *Microvasc Res* **72**, 161–171.

[21] Baluk P, Tammela T, Ator E, Lyubynska N, Achen MG, Hicklin DJ, Jeltsch M, Petrova TV, Pytowski B, Stacker SA, et al. (2005). Pathogenesis of persistent lymphatic vessel hyperplasia in chronic airway inflammation. *J Clin Invest* **115**, 247–257.

[22] Cha HS, Bae EK, Koh JH, Chai JY, Jeon CH, Ahn KS, Kim J, and Koh EM (2007). Tumor necrosis factor-α induces vascular endothelial growth factor-C expression in rheumatoid synoviocytes. *J Rheumatol* **34**, 16–19.

[23] Ristimaki A, Narko K, Enholm B, Joukov V, and Alitalo K (1998). Proinflammatory cytokines regulate expression of the lymphatic endothelial mitogen vascular endothelial growth factor-C. *J Biol Chem* **273**, 8413–8418.

[24] Shin HY, Smith ML, Toy KJ, Williams PM, Bizios R, and Gerritsen ME (2002). VEGF-C mediates cyclic pressure–induced endothelial cell proliferation. *Physiol Genomics* **11**, 245–251.

[25] Sharma P, Singh DP, Fatma N, Chylack LT Jr, and Shinohara T (2000). Activation of *LEDGF* gene by thermal- and oxidative-stresses. *Biochem Biophys Res Commun* **276**, 1320–1324.

[26] Zhang D, Wong LL, and Koay ES (2007). Phosphorylation of Ser78 of Hsp27 correlated with HER-2/*neu* status and lymph node positivity in breast cancer. *Mol Cancer* **6**, 52.

[27] Cohen-Kaplan V, Naroditsky I, Zetser A, Ilan N, Vlodavsky I, and Doweck I (2008). Heparanase induces VEGF C and facilitates tumor lymphangiogenesis. *Int J Cancer* **123**, 2566–2573.

[28] Machnik A, Neuhofer W, Jantsch J, Dahlmann A, Tammela T, Machura K, Park JK, Beck FX, Muller DN, Derer W, et al. (2009). Macrophages regulate salt-dependent volume and blood pressure by a vascular endothelial growth factor-C–dependent buffering mechanism. *Nat Med* **15**, 545–552.

[29] Shinohara T, Singh DP, and Fatma N (2002). LEDGF, a survival factor, activates stress-related genes. *Prog Retin Eye Res* **21**, 341–358.

[30] Nguyen TA, Boyle DL, Wagner LM, Shinohara T, and Takemoto DJ (2003). LEDGF activation of PKCγ and gap junction disassembly in lens epithelial cells. *Exp Eye Res* **76**, 565–572.

[31] Ganapathy V and Casiano CA (2004). Autoimmunity to the nuclear autoantigen DFS70 (LEDGF): what exactly are the autoantibodies trying to tell us? *Arthritis Rheum* **50**, 684–688.

[32] Daniels T, Zhang J, Gutierrez I, Elliot ML, Yamada B, Heeb MJ, Sheets SM, Wu X, and Casiano CA (2005). Antinuclear autoantibodies in prostate cancer: immunity to LEDGF/p75, a survival protein highly expressed in prostate tumors and cleaved during apoptosis. *Prostate* **62**, 14–26.

[33] Daugaard M, Kirkegaard-Sorensen T, Ostenfeld MS, Aaboe M, Hoyer-Hansen M, Orntoft TF, Rohde M, and Jaattela M (2007). Lens epithelium–derived growth factor is an Hsp70-2 regulated guardian of lysosomal stability in human cancer. *Cancer Res* **67**, 2559–2567.

[34] Poeschla EM (2008). Integrase, LEDGF/p75 and HIV replication. *Cell Mol Life Sci* **65**, 1403–1424.

[35] Singh DP, Kubo E, Takamura Y, Shinohara T, Kumar A, Chylack LT Jr, and Fatma N (2006). DNA binding domains and nuclear localization signal of LEDGF: contribution of two helix-turn-helix (HTH)–like domains and a stretch of 58 amino acids of the N-terminal to the trans-activation potential of LEDGF. *J Mol Biol* **355**, 379–394.

[36] Turlure F, Maertens G, Rahman S, Cherepanov P, and Engelman A (2006). A tripartite DNA-binding element, comprised of the nuclear localization signal and two AT-hook motifs, mediates the association of LEDGF/p75 with chromatin *in vivo*. *Nucleic Acids Res* **34**, 1653–1675.

[37] Maertens GN, Cherepanov P, and Engelman A (2006). Transcriptional co-activator p75 binds and tethers the Myc-interacting protein JPO2 to chromatin. *J Cell Sci* **119**, 2563–2571.

[38] Hobbs S, Jitrapakdee S, and Wallace JC (1998). Development of a bicistronic vector driven by the human polypeptide chain elongation factor 1α promoter for creation of stable mammalian cell lines that express very high levels of recombinant proteins. *Biochem Biophys Res Commun* **252**, 368–372.

[39] Vandekerckhove L, Christ F, Van Maele B, De Rijck J, Gijsbers R, Van den Haute C, Witvrouw M, and Debyser Z (2006). Transient and stable knockdown of the integrase cofactor LEDGF/p75 reveals its role in the replication cycle of human immunodeficiency virus. *J Virol* **80**, 1886–1896.

[40] Papenfuss HD, Gross JF, Intaglietta M, and Treese FA (1979). A transparent access chamber for the rat dorsal skin fold. *Microvasc Res* **18**, 311–318.

[41] Huang Q, Shan S, Braun RD, Lanzen J, Anyrhambatla G, Kong G, Borelli M, Corry P, Dewhirst MW, and Li CY (1999). Noninvasive visualization of tumors in rodent dorsal skin window chambers. *Nat Biotechnol* **17**, 1033–1035.

[42] Fukumura D and Jain RK (2008). Imaging angiogenesis and the microenvironment. *APMIS* **116**, 695–715.

[43] Kalchenko V, Brill A, Bayewitch M, Fine I, Zharov V, Galanzha E, Tuchin V, and Harmelin A (2007). *In vivo* dynamic light scattering imaging of blood coagulation. *J Biomed Opt* **12**, 052002.

[44] Kalchenko V, Preise D, Bayewitch M, Fine I, Burd K, and Harmelin A (2007). *In vivo* dynamic light scattering microscopy of tumour blood vessels. *J Microsc* **228**, 118–122.

[45] Smith TG Jr, Lange GD, and Marks WB (1996). Fractal methods and results in cellular morphology—dimensions, lacunarity and multifractals. *J Neurosci Methods* **69**, 123–136.

[46] Chan PK and Cheng SH (2003). Fractal analysis of vascular complexity in cadmium-treated zebrafish embryos. *Aquat Toxicol* **63**, 83–87.

[47] Kirchner LM, Schmidt SP, and Gruber BS (1996). Quantitation of angiogenesis in the chick chorioallantoic membrane model using fractal analysis. *Microvasc Res* **51**, 2–14.

[48] Lazarovici P, Gazit A, Staniszewska I, Marcinkiewicz C, and Lelkes PI (2006). Nerve growth factor (NGF) promotes angiogenesis in the quail chorioallantoic membrane. *Endothelium* **13**, 51–59.

[49] McKay TL, Gedeon DJ, Vickerman MB, Hylton AG, Ribita D, Olar HH, Kaiser PK, and Parsons-Wingerter P (2008). Selective inhibition of angiogenesis in small blood vessels and decrease in vessel diameter throughout the vascular tree by triamcinolone acetonide. *Invest Ophthalmol Vis Sci* **49**, 1184–1190.

[50] Parsons-Wingerter P, Lwai B, Yang MC, Elliott KE, Milaninia A, Redlitz A, Clark JI, and Sage EH (1998). A novel assay of angiogenesis in the quail chorioallantoic membrane: stimulation by bFGF and inhibition by angiostatin according to fractal dimension and grid intersection. *Microvasc Res* **55**, 201–214.

[51] Vickerman MB, Keith PA, McKay TL, Gedeon DJ, Watanabe M, Montano M, Karunamuni G, Kaiser PK, Sears JE, Ebrahem Q, et al. (2009). VESGEN 2D: automated, user-interactive software for quantification and mapping of angiogenic and lymphangiogenic trees and networks. *Anat Rec (Hoboken)* **292**, 320–332.

[52] Fatma N, Singh DP, Shinohara T, and Chylack LT Jr (2001). Transcriptional regulation of the *antioxidant protein 2* gene, a thiol-specific antioxidant, by lens epithelium–derived growth factor to protect cells from oxidative stress. *J Biol Chem* **276**, 48899–48907.

[53] Singh DP, Fatma N, Kimura A, Chylack LT Jr, and Shinohara T (2001). LEDGF binds to heat shock and stress-related element to activate the expression of stress-related genes. *Biochem Biophys Res Commun* **283**, 943–955.

[54] Kent WJ, Sugnet CW, Furey TS, Roskin KM, Pringle TH, Zahler AM, and Haussler D (2002). The human genome browser at UCSC. *Genome Res* **12**, 996–1006.

[55] Osato N, Suzuki Y, Ikeo K, and Gojobori T (2007). Transcriptional interferences in *cis* natural antisense transcripts of humans and mice. *Genetics* **176**, 1299–1306.

[56] Semenza GL (2007). Hypoxia-inducible factor 1 (HIF-1) pathway. *Sci STKE* **2007**, cm8.

[57] Cueni LN and Detmar M (2006). New insights into the molecular control of the lymphatic vascular system and its role in disease. *J Invest Dermatol* **126**, 2167–2177.

[58] Su JL, Yen CJ, Chen PS, Chuang SE, Hong CC, Kuo IH, Chen HY, Hung MC, and Kuo ML (2007). The role of the VEGF-C/VEGFR-3 axis in cancer progression. *Br J Cancer* **96**, 541–545.

[59] Ganapathy V, Daniels T, and Casiano CA (2003). LEDGF/p75: a novel nuclear autoantigen at the crossroads of cell survival and apoptosis. *Autoimmun Rev* **2**, 290–297.

[60] Van Maele B, Busschots K, Vandekerckhove L, Christ F, and Debyser Z (2006). Cellular co-factors of HIV-1 integration. *Trends Biochem Sci* **31**, 98–105.

[61] Morerio C, Acquila M, Rosanda C, Rapella A, Tassano E, Micalizzi C, and Panarello C (2005). t(9;11)(p22;p15) with NUP98-LEDGF fusion gene in pediatric acute myeloid leukemia. *Leuk Res* **29**, 467–470.

[62] Yokoyama A and Cleary ML (2008). Menin critically links MLL proteins with LEDGF on cancer-associated target genes. *Cancer Cell* **14**, 36–46.

[63] Moyano JV, Evans JR, Chen F, Lu M, Werner ME, Yehiely F, Diaz LK, Turbin D, Karaca G, Wiley E, et al. (2006). αB-Crystallin is a novel oncoprotein that predicts poor clinical outcome in breast cancer. *J Clin Invest* **116**, 261–270.

[64] Maertens GN, Cherepanov P, and Engelman A (2006). Transcriptional co-activator p75 binds and tethers the Myc-interacting protein JPO2 to chromatin. *J Cell Sci* **119**, 2563–2571.

[65] Sutherland HG, Newton K, Brownstein DG, Holmes MC, Kress C, Semple CA, and Bickmore WA (2006). Disruption of ledgf/psip1 results in perinatal mortality and homeotic skeletal transformations. *Mol Cell Biol* **26**, 7201–7210.

[66] Lopez-Lazaro M (2007). Dual role of hydrogen peroxide in cancer: possible relevance to cancer chemoprevention and therapy. *Cancer Lett* **252**, 1–8.

[67] Bonello S, Zahringer C, BelAiba RS, Djordjevic T, Hess J, Michiels C, Kietzmann T, and Gorlach A (2007). Reactive oxygen species activate the HIF-1α promoter via a functional NFκB site. *Arterioscler Thromb Vasc Biol* **27**, 755–761.

[68] Sawaji Y, Sato T, Takeuchi A, Hirata M, and Ito A (2002). Anti-angiogenic action of hyperthermia by suppressing gene expression and production of tumour-derived vascular endothelial growth factor *in vivo* and *in vitro*. *Br J Cancer* **86**, 1597–1603.

[69] Vanhee-Brossollet C and Vaquero C (1998). Do natural antisense transcripts make sense in eukaryotes? *Gene* **211**, 1–9.

[70] Herbert A (2004). The four Rs of RNA-directed evolution. *Nat Genet* **36**, 19–25.

[71] Lapidot M and Pilpel Y (2006). Genome-wide natural antisense transcription: coupling its regulation to its different regulatory mechanisms. *EMBO Rep* **7**, 1216–1222.

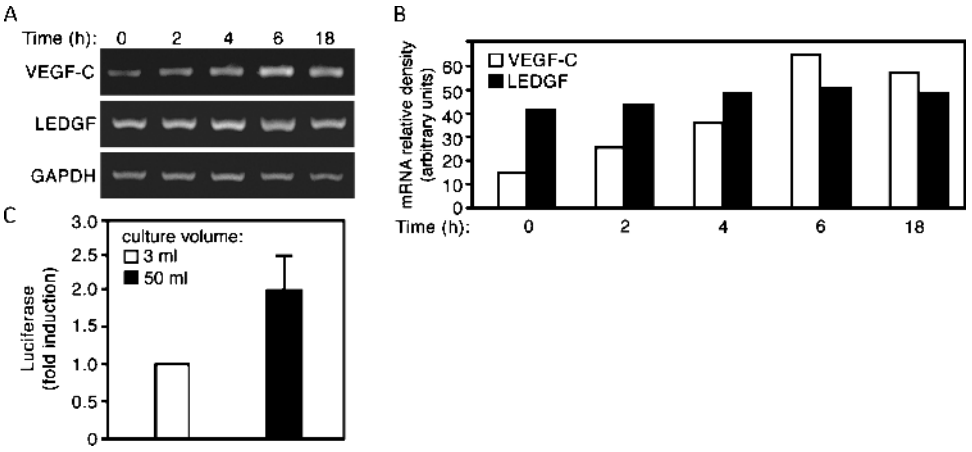

Figure W1. VEGF-C expression is induced by elevated culture medium pressure. (A) VEGF-C and LEDGF/p75 mRNA expression was analyzed by RT-PCR analysis in H1299 human lung cancer cells maintained in elevated column of culture medium (50 ml/1.1 cm) for the indicated time. (B) Relative intensity of the bands normalized against GAPDH. (C) Luciferase assay carried out with H1299 cells transiently transfected with pVEGF-Cwt-Luc reporter and cultured either in 3-ml (0.2 cm) or in high 50-ml culture medium (mean ± SD, $n = 3$).

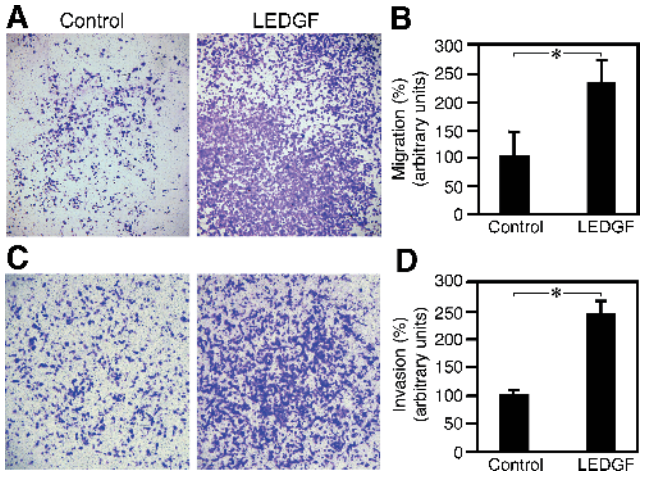

Figure W2. Overexpression of LEDGF/p75 augments migration and invasion rate of H1299 lung cancer cell *in vitro*. (A) Cell migration assay carried out *in vitro* with H1299 encoding the p75 variant of LEDGF (LEDGF) and control cells expressing an empty vector (Control). (B) Density of cells that had migrated through the filter. (C) Invasion of H1299 encoding LEDGF (LEDGF) and control cells (Control) through Matrigel. Cells were plated in transwell invasion chambers coated with Matrigel, and 12 hours later, cells that had migrated through the filter were stained. (D) Density of cells that invaded through the Matrigel. Three independent experiments were each carried out with at least triplicates, *$P < .01$.

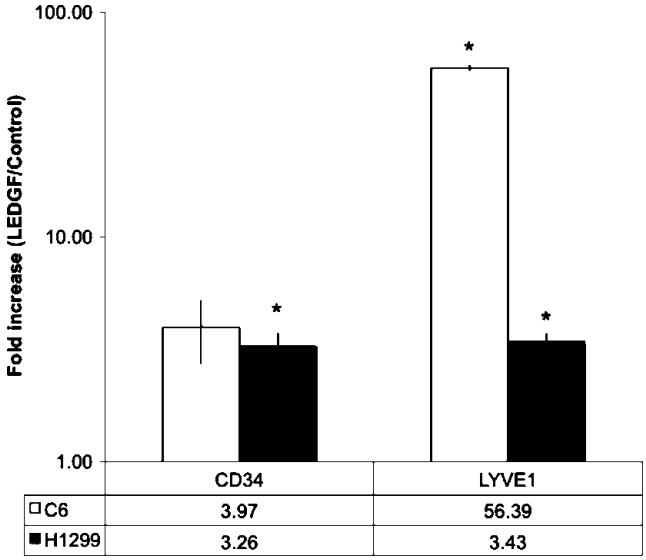

Figure W3. Ectopic expression of LEDGF/p75 augments blood and lymphatic vessels' quantity in H1299 and C6 tumors. The impact of LEDGF/p75 overexpression on blood and lymphatic vessels density was evaluated in the tumors described in Figures 5 and 6. Angiogenesis and lymphangiogenesis rates were deduced by counting the number of blood and lymphatic vessels after immunohistochemical staining using either antibodies against CD34 or LYVE-1, respectively. Data are presented as mean ± SD for fold induction of LEDGF/p75 over control tumors from at least three different tumors from each group normalized to the tumor section area (note the log scale of vessel density fold induction; *$P < .05$).

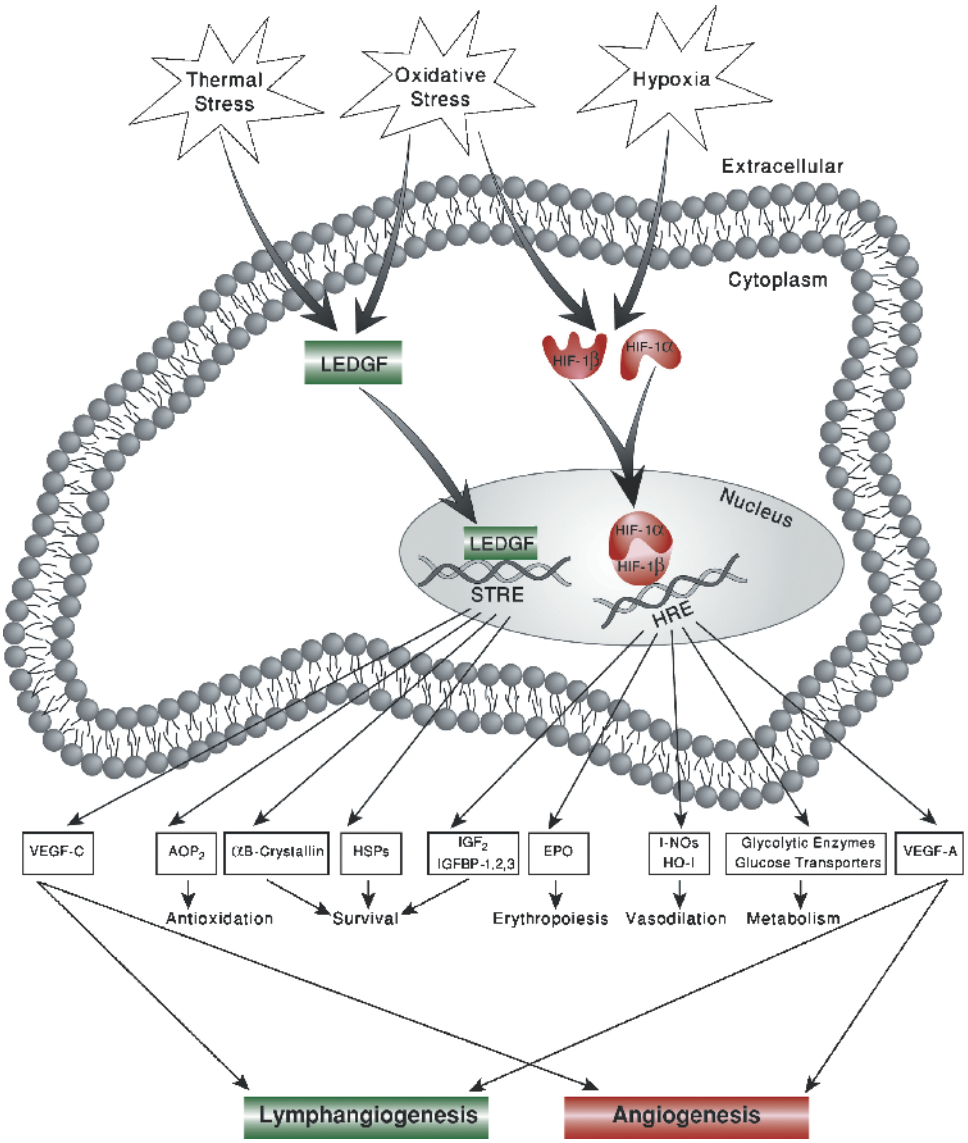

Figure W4. Microenvironmental control of tumor angiogenesis and lymphangiogenesis by LEDGF/p75. Angiogenesis and lymphangiogenesis are two complementary processes that play a vital role in physiological and pathologic circumstances. A key regulator of angiogenesis is the HIF-1 that is activated by hypoxia and oxidative stress. HIF-1 activates the transcription of hypoxia response element–containing genes involved in diverse aspects of cellular and integrative physiology, including energy metabolism (glycolytic enzymes and glucose transporters), survival (insulin-like growth factor 2 [IGF-2] and IGF-binding protein [IGFBP] 1,2,3), erythropoiesis (EPO), vasodilation (inducible nitric oxide synthase [I-NOS] and heme oxygenase 1 [HO-1]), and angiogenesis (VEGF, VEGF receptor fms-related kinase 1 [FLT-1]). In analogy, we show here that LEDGF is elevated by various stress signals including oxidative stress and hyperthermia. LEDGF confers its activity through binding to specific promoter elements (STRE and/or HSE) of many stress-related genes known to be involved in survival (heat shock proteins [HSPs], αB-crystallin) and in antioxidation (antioxidant protein 2 [AOP2]) and activates them. We propose here that LEDGF regulates lymphangiogenesis by mediating stress-induced expression of VEGF-C.